

## Three Phase Voltage Source Soft Switching Inverter with High Frequency Pulse Current Transformers

Claudio Y. Inaba, Eiji Hiraki, and Mutsuo Nakaoka\*

The Graduate School of Science & Engineering, Yamaguchi University, Yamaguchi, Japan

### ABSTRACT

In this paper, a high frequency transformer - assisted auxiliary active resonant commutated snubber (HFTA-ARCS) for voltage source soft switching pulse width modulated power conversion circuits is presented. A three phase voltage source type soft switching inverter incorporating HFTA-ARCS circuits in its three bridge legs can reduce current rating of auxiliary active power switches and has sensorless simplified control scheme which any specified boost current management is not required for soft switching. Its operation principle and digital control scheme are described and a practical design method of circuit parameters on this HFTA-ARCS circuit is also introduced on the basis of computer simulation. Moreover, this space voltage vector modulated soft switching inverter system with DSP-based digital control scheme is discussed and its effectiveness is proved on the basis of performance evaluations. The operating performances of this inverter system are also compared with those of conventional three-phase hard switching inverter under practical conditions of specified parameters.

**Keywords:** Three phase voltage source inverter, Soft switching, High frequency pulse current transformer - assisted auxiliary resonant snubbers, Space vector modulation, High power applications, DSP-based control scheme

### 1. Introduction

With great advances of power semiconductor devices and modules such as MOSFETs, IGBTs, IEGTs, SITs and SITHs, high switching frequency PWM schemes for voltage source type inverters and converters with a variety of digital control implementations are essentially indispensable for reducing the physical size, weight and total cost of equipment in addition to achieving their high

performances in transient and steady states. However, in conventional voltage source type hard switching PWM inverters and converters, switching power losses of power semiconductor devices and modules utilized become larger as well as  $dv/dt$  and  $di/dt$  related EMI noises. In addition, some serious problems such as the electrical insulation breakdown due to a high  $di/dt$  capability, the increase of leak current due to a high  $dv/dt$  and its related electric corrosion of bearing in AC motors driven by inverters using high frequency switching PWM strategies also become greater for high power applications.

A variety of power conversion circuits and systems topologies for applications in industrial power plants and renewal energy systems used as dispersed power supply

---

Manuscript received March 4, 2002; revised May 1, 2002.

Corresponding Author: nakaoka@pe-news1.eee.yamaguchi-u.ac.jp, Tel: +81-836-85-9472, Fax: +81-836-85-9401

have been investigated in some attractive attempts to solve the practical problems mentioned above; and soft switching PWM circuit technologies for high power inverters, rectifiers and DC-DC power converters have attracted special interest recently.

This paper presents the operation performances of an advanced type of active resonant commutated snubber<sup>[2]-[7]</sup>; high frequency transformer - assisted auxiliary resonant commutated snubber (HFTA-ARCS), which includes simplified control implementation with sensorless scheme and reduced auxiliary circuit device voltage and current stresses. The operation principle of the three phase voltage source type space voltage vector modulated soft commutation inverter with a type 1 optimal digital servo control scheme which respectively incorporates HFTA-ARCS into its three phase bridge legs is described on the basis of performance evaluations. The operation performances of this inverter system for high power applications are compared with those of conventional hard switching three-phase inverter under practical conditions of specified parameters.

## 2. Auxiliary Resonant Snubber with High-Frequency Transformer

### 2.1 Circuit Topology

The one-arm topology of the auxiliary active resonant commutated snubber with a high frequency transformer is shown in Fig. 1.

This resonant snubber circuit is composed of two auxiliary active power switches ( $S_{a1}, S_{a2}$ );

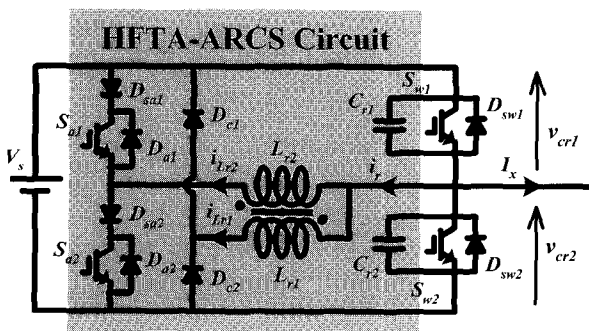


Fig. 1. Circuit diagram of the high frequency transformer – assisted auxiliary resonant commutated snubber (HFTA-ARCS).

two resonant capacitors ( $C_{r1}, C_{r2}$ ); two current feedback diodes ( $D_{c1}, D_{c2}$ ) connected to the primary side resonant inductor  $L_{r1}$  of high frequency transformer ( $L_{r1}, L_{r2}$ ) and two additional reverse blocking diodes ( $D_{sa1}, D_{sa2}$ ) which block the freewheeling current path composed by its secondary side inductor  $L_{r2}$  and freewheeling diode  $D_{a1}$  or  $D_{a2}$ , depending on the switching transition<sup>[4]</sup>.

### 2.2 Operation Principle

Considering that all the switching power devices are ideal and load current  $I_x$  is kept constant during the short commutation interval, the operation principle of HFTA-ARCS circuit is represented below:

Voltage and current waveforms of main active power switching blocks  $Q_1(S_{w1}/D_{sw1}), Q_2(S_{w2}/D_{sw2})$  and current waveforms for the primary and secondary winding of high frequency transformer are represented in Fig. 2 when load current  $I_x$  as a current source flows to the positive direction; and each operation stage of this circuit is shown in Fig. 3.

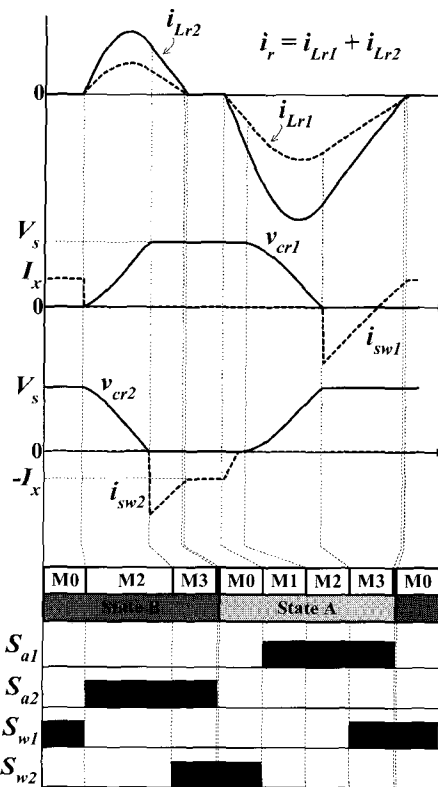


Fig. 2. Operation waveforms of HFTA-ARCS and its switching drive signals.

The operation principle of HFTA-ARCS circuit in a steady state is described as follows:

**(a) State A: Mode 0**

The active power switch  $S_{w2}$  is on and  $S_{w1}$  is off, when load current  $I_x$  with a positive direction flows through  $D_{sw2}$ .

**(b) State A: Mode 1**

The auxiliary active power switch  $S_{a1}(D_{sa1})$  is turned on under a principle of ZCS condition and  $S_{w2}$  is turned off under a principle of ZVS condition. The transformer secondary side inductor current  $i_{Lr2}$  begins to increase linearly with a certain slope and its primary side inductor current  $i_{Lr1}$  also begins to increase, because of the mutual inductance  $M$  existed between  $L_{r1}$  and  $L_{r2}$ .  $D_{c2}$  turns on. Current flowing through  $D_{sw2}$  starts decreasing. When  $i_r \leq -I_x$ , the current in  $D_{sw2}$  becomes zero and this mode completes.

**(c) State A: Mode 2**

Resonance based on the leakage inductance of high frequency transformer and resonant capacitors ( $C_{r1}$ ,  $C_{r2}$ ) starts partially. Voltage across  $C_{r1}$  is discharged to zero and voltage across  $C_{r2}$  is charged to  $V_s$ . It is noted that any specified boost current of this resonant snubber for soft switching is not necessary in mode 1 because the energy stored in the leakage inductance of high frequency transformer will be large enough to charge and discharge the quasi-resonant capacitors. In this case, the turn-ratio of high frequency transformer should be adequately designed so as to be  $L_{r1} \geq L_{r2}$ .

**(d) State A: Mode 3-1**

When  $v_{cr1}$  becomes zero,  $D_{sw1}$  turns on and resonant current  $i_r$  starts decreasing linearly towards the negative direction.

**(e) State A: Mode 3-2**

At the same instant when current in  $D_{sw1}$  reaches zero,  $(i_r + I_x) \geq 0$ ,  $S_{w1}$  turns on under both ZVS and ZCS. The next operation mode reveals at the instant when  $i_{Lr1}$  reaches zero. As a result  $D_{c2}$  turns off.

**(f) State A: Mode 4**

Some current still remains in  $L_{r2}$  and when  $i_r \approx 0$ ,  $S_{a1}$  is turned off. The load current  $I_x$  is totally transferred to  $S_{w1}$ .

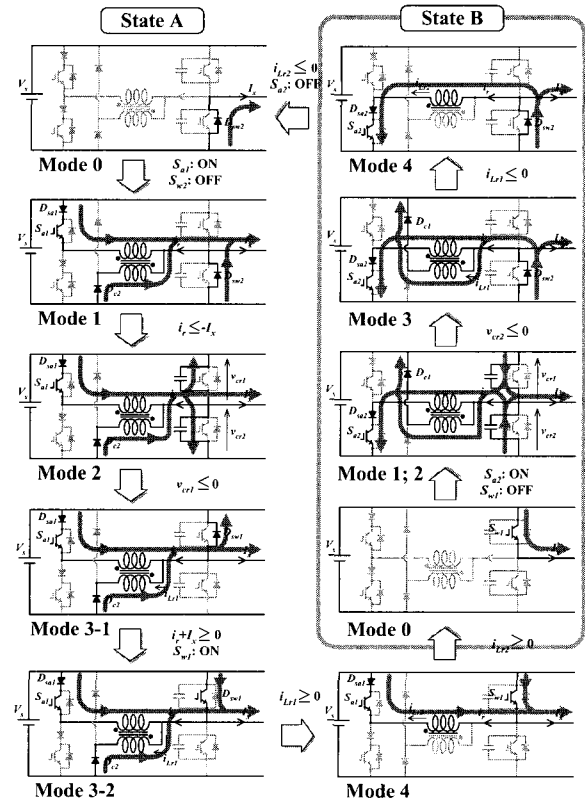


Fig. 3. Equivalent circuit for each commutation stage of HFTA-ARCS circuit.

**(g) State B: Mode 0**

$S_{w2}$  is off and  $I_x$  flows through  $S_{w1}$ .

**(h) State B: Mode 1, 2**

$S_{w1}$  is turned off and  $S_{a2}$  is turned on simultaneously. Since any boost current is not necessary, resonance based on the leakage inductor of high frequency transformer and resonant capacitors starts. Voltage across  $C_{r2}$  is discharged to zero and voltage across  $C_{r1}$  is charged to  $V_s$ .

**(i) State B: Mode 3**

When  $v_{cr2}$  becomes zero,  $D_{sw2}$  is turned on and the resonant current  $i_r$  starts decreasing linearly. The next operation mode reveals at the instant when  $i_{Lr1}$  reaches zero. As a result  $D_{c1}$  turns off.

**(j) State B: Mode 4**

The resonant current  $i_r$  still continues decreasing. When  $i_r \approx 0$ ,  $S_{a2}$  is turned off. The load current  $I_x$  is totally transferred to  $D_{sw2}$ . As a result, the commutation stage goes back to State A - Mode 0.

### 3. Practical Design Procedure of the Auxiliary Resonant Snubber

Considering the turn-ratio of high frequency transformer as  $N=n_2/n_1$  ( $n_1, n_2$ : number of turns at primary and secondary sides); setting  $N<1$  is indispensable in order to achieve a soft switching mode transition.

The circuit parameters of HFTA-ARCS in Fig. 1 are designed for a  $P_{out}=50\text{kW}$  three-phase inverter system with a DC source voltage  $V_s=400\text{V}$ . The specified output line voltage  $V_{ref}$  and sampling frequency  $f_s$  are  $200\text{V}_{\text{rms}}$  and  $12\text{kHz}$ , respectively. In addition, the practical conditions (a) and (b) indicated below must be met in order to select optimum parameters;

(a) Minimum current stresses in the auxiliary active power switches.

(b) Maximum commutation interval  $t_c$ , in this case, is to be designed at  $1/10$  of one sampling period  $T_s=1/f_s$ .

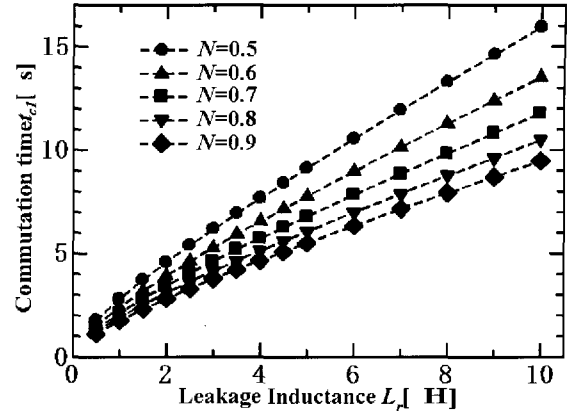
Each circuit parameter, which meets conditions (a) and (b) mentioned above, is designed by the following illustrative methods:

(i) Maximum output current for resistive load  $I_{max} \cong 205\text{A}$  is calculated from Eq. (1), using the values  $V_{ref}$  and  $P_{out}$  mentioned above. In this case, the power factor is  $\cos\theta = 1$ . Considering that load line current  $I_x$  in Fig. 1 is kept constant; in this case  $I_x=210\text{A}$ , the commutation interval ( $t_{c1}, t_{c2}$ ) and peak current ( $I_{peak1}, I_{peak2}$ ) of the auxiliary active power switch in relation to the leakage inductance of high frequency transformer are to be determined; and these results are shown in Fig. 4 and Fig. 5, respectively.

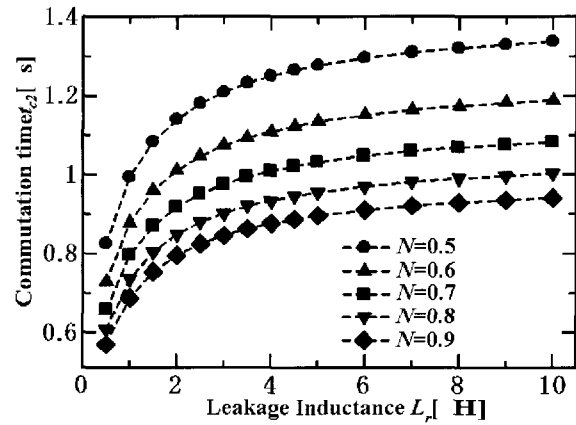
$$I_{max} = \sqrt{\frac{2}{3}} \cdot \frac{P_{out}}{V_{ref} \cos\theta} \quad (1)$$

(ii) The coupling coefficient  $k$  of the high frequency transformer is set to 0.99.

(iii) The resonant capacitor  $C_r$  is set to  $0.25\mu\text{F}$ . In the case that this value becomes large, the commutation period increases. As a result, the inverter efficiency is actually deteriorated. In the case that  $C_r$  is smaller than  $0.25\mu\text{F}$ , soft switching effect can be reduced. So, the maximum  $dv/dt$  is to be set to  $500\text{V}/\mu\text{s}$ .



(a) State A



(b) State B

Fig. 4. Commutation time in relation to leakage inductance and turn ratio of high frequency transformer.

(iv) Observing Fig. 4(a), it is concluded that the leakage inductance  $L_r$  of high frequency transformer, when turn-ratio  $N$  is 0.9, should be less than  $9\mu\text{H}$  in order to meet the practical condition specified in (b) since one sampling period  $T_s$  is  $83.3\mu\text{s}$ . And more, from Fig. 5(a), it is concluded that the design value of  $L_r$  should be higher than  $3\mu\text{H}$  in order to meet the required condition which is specified in (a) mentioned above.

Although peak current of auxiliary active switch changes according to  $N$  as depicted in Fig. 5, the value of resonant peak current is the same even turn-ratio  $N$  changes.

This practical design procedure explained from (i) to (iv) can be summarized through the flow chart illustrated in Fig. 6.

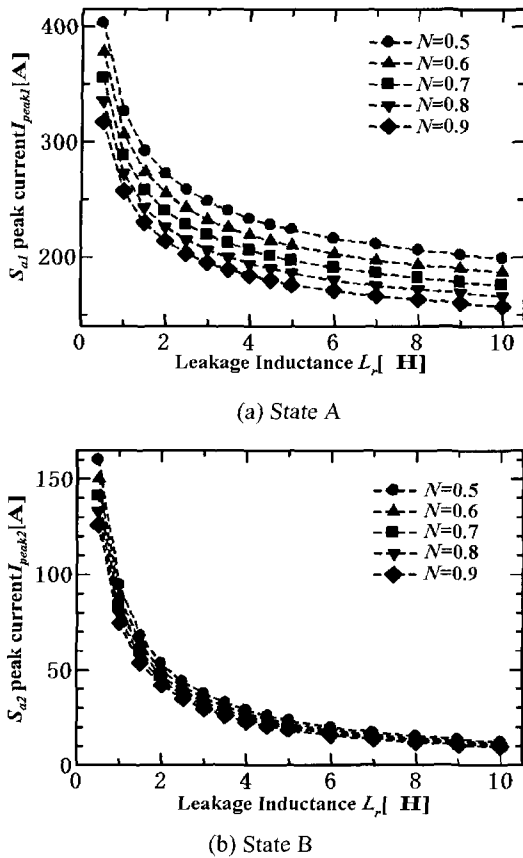


Fig. 5. Peak current of auxiliary switch in relation to leakage inductance of high frequency transformer.

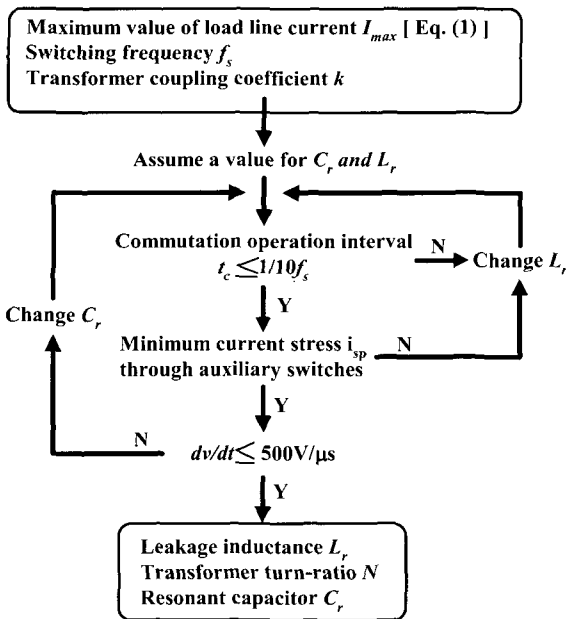


Fig. 6. Design procedure of auxiliary quasi-resonant snubber.

### 4. Three Phase Soft Commutation PWM Inverter and Its Control Scheme

#### 4.1 System Configuration of Soft Switching Inverter

Fig. 7 shows the voltage source three phase soft switching inverter with high frequency transformer – assisted resonant commutation snubbers and the optimal type 1 servo digital control implementation for this inverter is illustrated in Fig. 8.

In every sampling time, instantaneous three phase voltage vectors  $v_c(t)$  and three phase filter inductor current vectors  $i_A(t)$  are detected respectively by voltage and current sensors. In order to reduce system variables,  $v_c(t)$  and  $i_A(t)$  values are changed to the  $\alpha$ - $\beta$  stationary coordinate plane and then changed to the  $d$ - $q$  synchronous rotating coordinate plane. As a result, from the variables on the  $d$ - $q$  synchronous rotating coordinate plane,

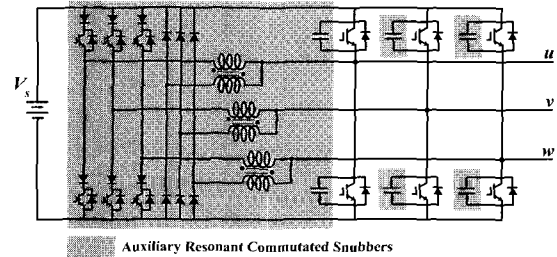


Fig. 7. Circuit diagram of three-phase voltage source soft switching inverter using high frequency transformers.

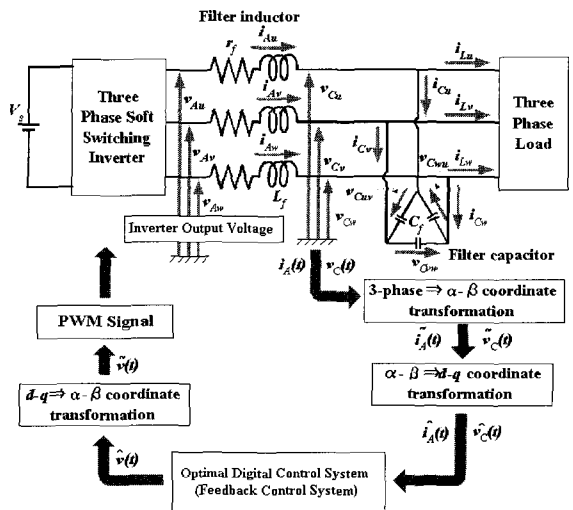


Fig. 8. Optimal digital control scheme of three phase soft switching inverter system.

the output voltage vector is specified at the feedback control system displayed in Fig. 8 and the output voltage vector is adequately calculated from this digital control process scheme.

Each designed parameter of the voltage source type three phase soft switching inverter system presented in this paper is indicated in Table 1. The resonant inductor  $L_r$  is estimated to be  $7\mu\text{H}$ . High frequency transformer primary side inductor  $L_1$ , its secondary side inductor  $L_2$  and their mutual inductance  $M$  are calculated from Eq. (2) using parameters  $L_r$ ,  $k$  and  $N$ .

$$L_1 = \frac{k^2}{(1-k^2)N^2} L_r, \quad L_2 = \frac{1}{1-k^2} L_r, \quad M = \frac{k^2}{(1-k^2)N} L_r \quad (2)$$

Table 1. Design Specifications and Parameters of the Inverter System.

DC voltage source	$V_s$	400V
Sampling frequency	$f_s$	12kHz
Resonant capacitor	$C_r$	$0.25\mu\text{F}$
Leakage inductance	$L_r$	$7\mu\text{H}$
Self inductance of primary side inductor	$L_1$	$539\mu\text{H}$
Self inductance of secondary side inductor	$L_2$	$352\mu\text{H}$
Transformer mutual inductance	$M$	$431\mu\text{H}$
Transformer magnetic coupling coefficient	$k$	0.99
Turn-ratio	$N$	0.8
Self inductance of filter inductor	$L_f$	$206\mu\text{H}$
Filter capacitor	$C_f$	$85.3\mu\text{F}$
Output voltage [rms]	$V_{ref}$	200V
Output frequency	$f_{out}$	60Hz

Table 2. Load Circuit Parameters.

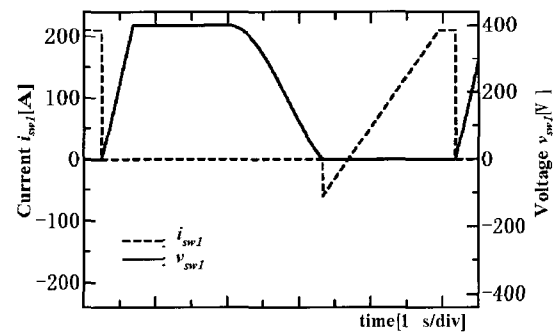
Load type		Value	
Resistive load		$0.85\Omega$	Star connection
Inductive load (power factor = 0.8)	Resistance	$0.70\Omega$	Star connection
	Inductance	$1100\mu\text{H}$	

The performance evaluations of this soft switching inverter system with a digital control scheme are carried out for resistive load and inductive load. Moreover, a voltage source type three-phase hard switching inverter with a dead time  $t_d=1.5\mu\text{s}$  utilizing the same parameters in comparing with the three phase soft switching inverter with resonant snubbers treated here is also analyzed and the comparative studies are performed for 50kW power supply. Table 2 shows the parameters of the three-phase load types.

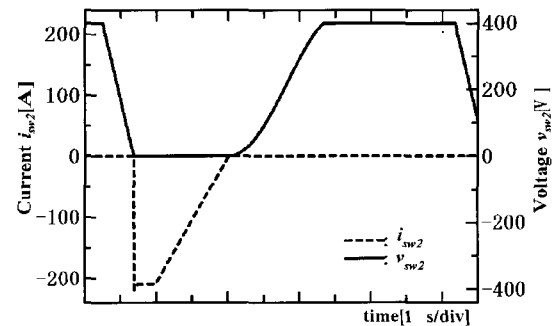
## 4.2 Simulation Results and Feasible Evaluations

Fig. 9 and Fig. 10 show the typical voltage and current operating waveforms of main and auxiliary active power switches when the parameters indicated in Table 1, are implemented. The operating voltage and current waveforms in Fig. 9 and Fig. 10 are obtained when  $I_x=210\text{A}$ .

The two topological types, hard switching space voltage vector modulated inverter and soft switching space voltage



(a) Highside main switch current and voltage waveforms



(b) Lowside main switch current and voltage waveforms

Fig. 9. Turn on and turn off waveforms of main switches.

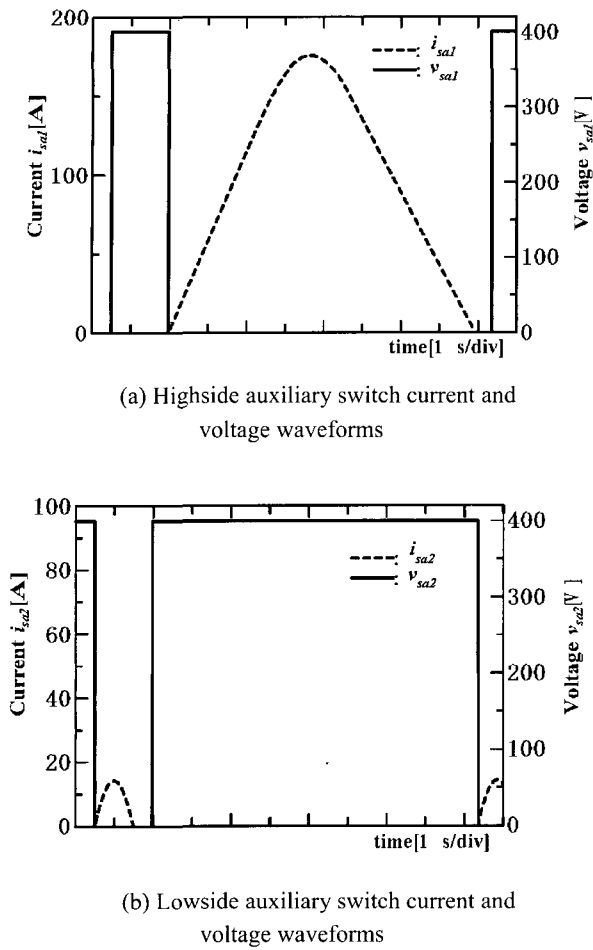
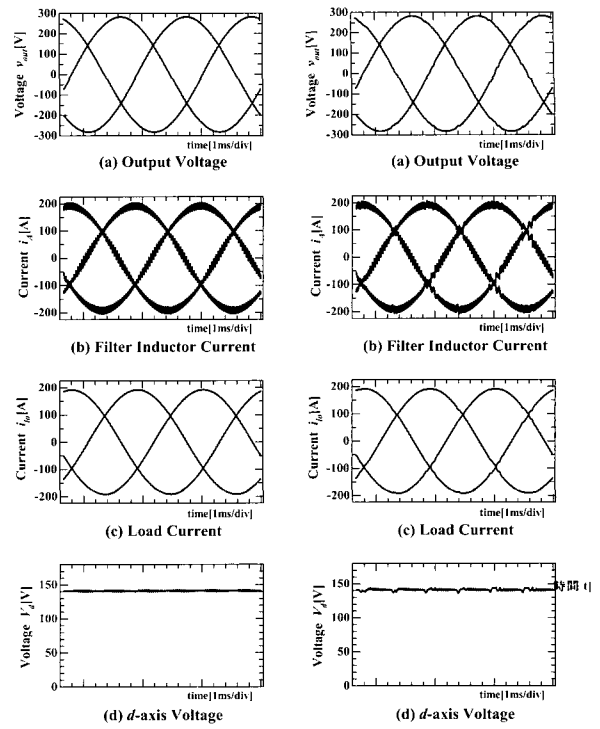


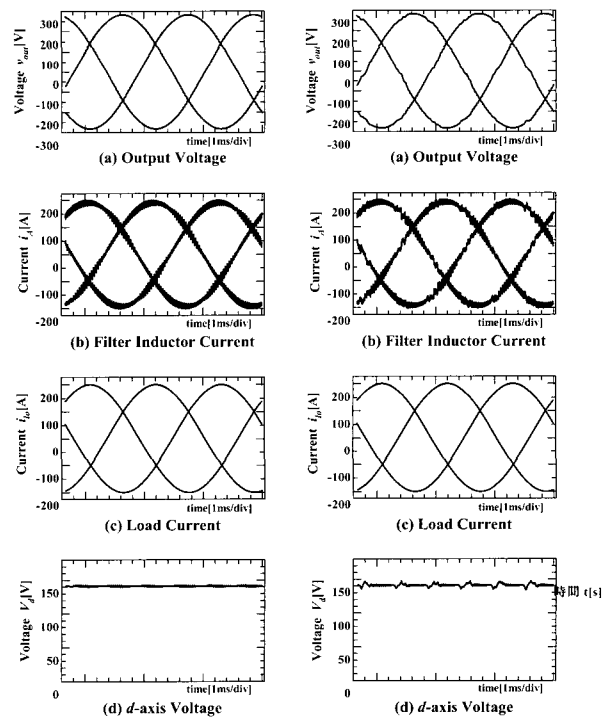
Fig. 10. Turn on and turn off waveforms of auxiliary switches.

vector modulated inverter; are applied to three phase balanced resistive and inductive loads and output voltage and current waveforms are illustrated in Fig. 11 and Fig. 12, respectively. Fig. 11(a) and Fig. 12(a) give the output line-to-line voltage. Fig. 11(b) and Fig. 12(b) give the filter inductor current. Figures 11(c) and 12(c) also depict the load current. And in Fig. 11(d) and Fig. 12(d),  $d$ -axis voltages for each topology are illustrated, respectively.

Total harmonic distortion (THD) of output voltage for each switching scheme is displayed in Table 3. From these results, it is concluded that THD of the output voltage waveform, when HFTA-ARCS circuit is effectively introduced, can be higher than the THD of voltage-fed three phase hard switching inverter system. However, soft switching mode transition can be achieved, reducing power losses of switching devices and EMI noises.



In case of hard switching  
 Fig. 11. Output waveforms of three-phase inverter with balanced resistive load.



In case of soft switching  
 Fig. 12. Output waveforms of three-phase inverter with balanced inductive load.

Table 3. Total Harmonic Distortion Factor–THD [%] of Output Voltage.

	Hard switching	Soft switching
Resistive load	0.477	0.942
Inductive load	0.533	1.376

## 5. Conclusions

This paper has presented the steady-state operating principle and salient features of the space voltage vector modulated three phase voltage source soft switching inverter with high frequency transformer – assisted auxiliary resonant commutation snubber (HFTA-ARCS) circuits operating under an optimal type I digital servo controller which tracks a specified output reference voltage. It was proved by performance evaluations that the prototype of 50kW three-phase voltage source soft switching inverter proposed here could efficiently work with high performances in order to minimize the power losses and EMI noises in active power switches. In addition to these, the optimum circuit design approach of HFTA-ARCS has been described on the basis of computer-aided analysis.

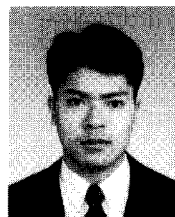
In the future, feasible studies on voltage-fed three phase soft switching inverter and power factor corrector converter systems with high frequency transformer - assisted auxiliary resonant commutation snubbers (HFTA-ARCS) using extremely lowered trench gate HV-IGBTs for high power applications should be investigated and evaluated from a practical point of view.

## References

- [1] R.W. De Doncker, "The Auxiliary Resonant Commutated Pole Converter", IEEE IAS Annual Meeting Records, Vol. 3, pp. 829~834, October 1989.
- [2] E. Hiraki, M. Ishibashi, M. Nakaoka, T. Horiuchi, and Y. Sugawara, "Feasible Performance Evaluations of Active Resonant Snubber-Assisted Three Phase Soft Switching Inverter", IEEE PESC CD-ROM, June 1999.
- [3] H. Yonemori, K. Hayashi, and M. Nakaoka, "A Novel

Space Voltage Vector Modulated Sinewave Three Phase Inverter with High Frequency Transformer Coupled Resonant DC Link", Proceedings of IEEE PESC, Vol. 2, pp. 651~658, June 1994.

- [4] X. Yuan and I. Barbi, "Control Simplification and Stress Reduction in a Modified PWM Zero Voltage Switching Pole Inverter", Proceedings of IEEE APEC, Vol. 3, pp. 1019~1025, March 1999.
- [5] C.Y. Inaba, Y. Hirota, Y. Konishi, E. Hiraki, and M. Nakaoka, "Practical Design Procedure of Resonant Snubber with Current Transformer and Performance Evaluations of a Digitally Controlled Three Phase Soft Switching Inverter", Proceedings of IEEE IAS Annual Meeting, Vol. 4, pp. 2448~2454, October 2001.
- [6] X. Yuan and I. Barbi, "Analysis, Designing and Experimentation of a Transformer-Assisted PWM Zero-Voltage Switching Pole Inverter", IEEE Trans. on Power Electronics, Vol. 15, No. 1 pp. 72~82, January 2000.
- [7] W. Dong, D. Peng, H. Yu, J. Lai, and F.C. Lee, "An Improved Zero-Voltage-Transition Inverter Using Coupled Inductors", Proceedings of IEE-Japan IPEC-Tokyo, Vol. 3, pp. 1621~1626, April 2000.
- [8] S. Sato, Y. Suehiro, S. Nagai, and K. Morita, "High Efficiency Soft Switching 3 Phase PWM Inverter", Proceedings of IEEE INTELEC, pp. 453~460, September 2000.
- [9] M. Kurokawa, C.Y. Inaba, Y. Konishi, H. Iwamoto, and M. Nakaoka, "Lossless Capacitive Snubber Assisted Auxiliary Resonant DC Link Voltage Source Soft Switching Inverter", Proceedings of IEEE PESC, Vol. 3, pp. 1233~1238, June 2000.
- [10] Y. Chen, "A New Quasi-Parallel Resonant DC Link for Soft Switching PWM Inverters", IEEE Trans. on Power Electronics, Vol. 13, No. 3 pp. 427~435, May 1998.



**Claudio Y. Inaba** received his B.S. and M.S. in Electrical and Electronics Engineering from Yamaguchi University, Japan in 2000 and 2002. He is currently doing research at Division of Electrical System Engineering, Yamaguchi University, Japan towards his Ph. D. degree. His research interests include soft switching PWM inverters and DC-DC converters for industrial applications. Mr. Inaba is a student member of IEE-Japan and IEEE-USA.





**Eiji Hiraki** was born in Yamaguchi, Japan. He received the M. Eng. degree from the Department of Electronics Engineering, Osaka University, Osaka, Japan in 1990. He is currently with the Power Electronic System and Control Engineering Laboratory at Yamaguchi University, Japan,

as a Research Associate. His research interests are in the Soft-switching Technique for High frequency switching Power Conversion systems. He is a member of the IEE, Japan.



**Mutsuo Nakaoka** was born in Hiroshima, Japan. He received his Ph. D degree in Electrical Engineering from Osaka University, Osaka, Japan in 1981. He joined in the Electrical and Electronics Engineering Department, Kobe University, Kobe, Japan in 1981. Since 1995, he has

been a professor in the Electrical and Electronics Engineering Department, the Graduate School of Engineering and Science, Yamaguchi University, Yamaguchi, Japan. His research interests include circuit and control systems of power electronics, especially in soft-switching areas. He is a member of the Institute of Electrical Engineers of Japan, the Institute of Electronics, Information and Communication Engineers of Japan, the Institute of Illumination Engineering of Japan and a senior member of IEEE.